COMMUNICATION

ChemComm
www.rsc.org/chemcomm

Magnetic nanochains of metal formed by assembly of small nanoparticles†

Chen-Min Liu,[a] Lin Guo,*[a,c] Rong-Ming Wang,*[b] Yuan Deng,[a] Hui-Bin Xu[a] and Shihe Yang*[c]

[a] *School of Material Science and Engineering, Beijing University of Aeronautics and Astronautics, Beijing 100083, China. E-mail: guolin@buaa.edu.cn; Fax: +86-10-82338162; Tel: +86-10-82338162*

[b] *Electron Microscopy Laboratory and State Key Laboratory for Mesoscopic Physics, Peking University, Beijing 100871, China. E-mail: rmwang@pku.edu.cn; Fax: +86-1062757551; Tel: +86-10-62757171*

[c] *Department of Chemistry, The Hong Kong University of Science and Technology, Clear Water Bay, Kowloon, Hong Kong, P. R. China. E-mail: chsyang@ust.hk; Fax: 852-2358-1594; Tel: (852) 2358-7362*

Received (in Cambridge, UK) 26th July 2004, Accepted 8th September 2004
First published as an Advance Article on the web 14th October 2004

Ni nanochains are synthesized with diameters of 150–250 nm and lengths of 0.5–2 μm by assembly of small nanoparticles, which exhibit a magnetic coercivity over two orders of magnitude larger than that of bulk Ni.

Although high yield syntheses of monodispersed magnetic nanoparticles have been achieved, simultaneous control of their shape, surface structure, and anisotropy is still a challenge. Currently, there is a genuine need for general approaches to fabricating low dimensional structures of magnetic metals through directed-assembly using nanoscale building blocks.[1] Surfactant-assisted shape-selective syntheses of nanostructured nickel colloid, nanoparticle agglomerates, submicron hollow spheres, and cobalt nanoparticle rings have been achieved.[2] Recently, Cordente *et al.*[3] have demonstrated the first synthesis of nickel nanorods by using HAD (hexadecylamine) as a shape-inducing agent instead of the conventional templates. In this communication, we report a simple solution-phase approach to the synthesis of pure nickel nanochains in the presence of a multidentate ligand poly(vinyl pyrrolidone) (PVP).

The Ni nanochains were grown by reduction of Ni^{2+} in a solution (see also S1). In brief, 5 ml ethylene glycol (EG) was heated to the boiling point (~195 °C) and refluxed for 5 min. Then, 1 ml of hydrazine monohydrate (50%, Vol. A.R.) was added dropwise to the boiling solution. 2 min later, 2.5 ml of $NiCl_2 \cdot 6H_2O$ solution (0.2 mol/l, in EG) and 5 ml of PVP solution (0.3 mol/l, in EG) were added rapidly to the boiling solution under vigorous magnetic stirring. After refluxing for about 60 min, the final products in the form of loose black powder were obtained by centrifugation. The powder was rinsed repeatedly with absolute ethanol for over 6 times, followed by the removal of the residual solvent through evaporation in vacuum at 80 °C. The yield of the Ni nanochains was as high as 80%. We noticed that no sign of oxidation was observed on the nickel nanochains we prepared even after aging for over 6 months under ambient conditions. This indicates that the nickel nanochains are very stable after surface modification with PVP, which is very important for future applications.

Fig. 1a shows the X-ray diffraction (XRD) pattern of a typical Ni nanochain sample. All of the diffraction peaks can be assigned to the Ni fcc structure (JCPDS 04-0850) and no impurity phases such as NiO or precursor compounds have been detected. The purity of the as-prepared network of the Ni nanoparticle chains is further verified by Energy Dispersive X-ray Spectroscopy (EDX). The result is shown in Fig. 1b, which exhibits appreciable signals only for Ni.

Information on the morphologies and structures of the Ni nanochains networks can be gleaned from Fig. 2. As shown in Fig. 2a, all of the Ni nanochains are in the size range of 150–250 nm

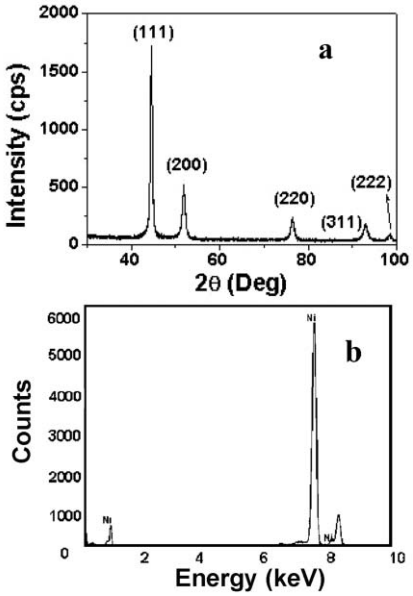

Fig. 1 a. XRD pattern of the as-synthesized nickel nanochain networks; b. EDX profile of a nickel nanochain of the as-synthesized sample.

and they are in close contact with each other, forming branched, necklace-like chains with lengths of 0.5–2 μm. This can be seen more clearly from the bright field TEM image in Fig. 2b. The corresponding nano-beam electron diffraction (NBED) pattern of the nickel nanochains network is displayed in the inset of the TEM image, which indicates that the nanoparticle network is polycrystalline. In fact, the individual nanoparticles are also found to be polycrystalline. The observed ED rings (see the inset of Fig. 2b) are converted to the lattice spacings of 0.203, 0.176, 0.124, and 0.106 nm, which are nicely indexed to the (111), (200), (220), and (311) planes of the fcc nickel, respectively. This is in complete agreement with the inference above from the XRD result. However, it is noticed that the NBED rings are not continuous but composed of discrete spots, which suggests preferential orientations of the Ni nanoparticles in the chain network.

Fig. 2c is a lattice-resolved HRTEM image taken near the contact region of two contiguous Ni nanoparticles (see also a more magnified view in Fig. S5). Obviously, the lattice fringes prolongate across the two nanoparticles without interruption by an apparent boundary. To our knowledge, such nearly epitaxially attached and fused Ni nanoparticle chains in a highly-branched network are unprecedented.

Regarding the mechanism for the growth of highly branched Ni nanoparticle chains, we believe that both $N_2H_4 \cdot H_2O$ and PVP play important roles. Most probably, $N_2H_4 \cdot H_2O$ serves both as a ligand and a reducing agent during the reaction. To start with, Ni^{2+} in the solution reacted with hydrazine to form sky-blue complex,

† Electronic supplementary information (ESI) available: synthesis, magnetic measurements, Ni nanoparticle to nanochain evolution, enlarged HRTEM image of Fig. 2c. See http://www.rsc.org/suppdata/cc/b4/b411311j/

DOI: 10.1039/b411311j

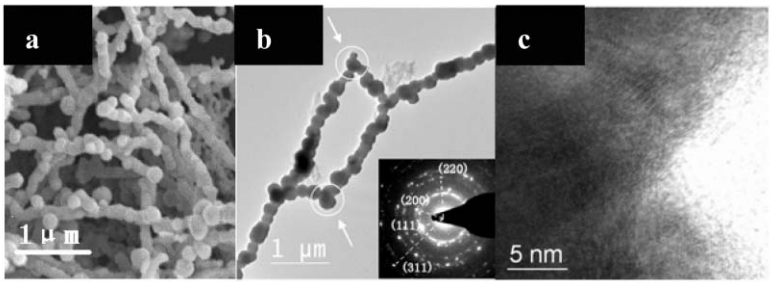

Fig. 2 a. SEM image of a typical as-prepared Ni nanochain sample; b. A bright field TEM image. The inset shows the corresponding nano-beam electron diffraction (NBED) pattern; c. A lattice-resolved HRTEM image taken near the joint region of two contiguous Ni nanoparticles.

$[Ni(N_2H_4)_3]^{2+}$, which is very stable at ambient temperature.[4] At the boiling point of ethylene glycol (about 197 °C), the excessive hydrazine acted as a reducing agent and converted $[Ni(N_2H_4)_3]^{2+}$ to Ni through homogeneous nucleation. The Ni nanoparticle formation is likely to involve the following chemical reactions:

$$Ni^{2+} + N_2H_4 \rightarrow [Ni(N_2H_4)_3]^{2+}$$

$$[Ni(N_2H_4)_3]^{2+} + N_2H_4 \rightarrow Ni\downarrow + 4NH_3\uparrow + 2N_2\uparrow + H_2\uparrow + 2H^+$$

At this time forward, the PVP molecules behaved like soft-templates. Initially, very small Ni nanoparticles (~10 nm) were formed (see Fig. S4). With the increase of the refluxing time, presumably, the small Ni nanoparticles diffused and aggregated to form larger nanoparticles due to the magnetic dipole–dipole interaction and effects of the PVP templates. The larger Ni nanoparticles were then assembled into necklace-like chains with multiple branches because of the stronger anisotropic magnetic forces. At the growth temperature, there was a thermodynamic driving force for aggregated growth because the surface energy is reduced substantially when the interface is eliminated.[5,6] The little lattice mis-orientation between the bordering Ni nanoparticles (Fig. 2c) suggests that an oriented attachment mechanism may also play a role at certain stages of the assembly as found for other systems.[7,8] In the synthesis of Ni nanochains, we often encountered trimmed Cayley Trees,[9] which can well explain the formation of the highly branched nanochains network. In the Cayley Trees, some of the branches have dead ends. This so happens when two growing branches stumble upon each other, blocking further growth.[10] In the highly-branched network of the Ni nanochains we prepared, such dead ends can be clearly seen, as indicated by arrows in Fig. 2b.

It should be mentioned that similar Co nanochains had also been prepared successfully using the same methods in our laboratory (see Fig. S3). This strongly suggests that our method is rather general for the synthesis of branched metal nanochain networks.

Magnetic properties of the branched Ni nanochains were investigated by a VSM (vibrating sample magnetometer) technique (see S2). The coercivity value amounts to 16 mT for Ni nanoparticle chains, which is over two orders of magnitude larger than that of bulk Ni (0.07 mT).[11] One can expect that the reduced size and dimensionality of the Ni nanostructures may change the magnetization reversal mechanism, leading to the large enhancement of coercivity. This is interesting for future application of magnetic recording devices. Second, the magnetization hysteresis loop is symmetric with respect to the zero field. This suggests that there is no exchange biasing effect[12] caused by, say, NiO (T_N = 520 K),[11] because the exchange coupling between ferromagnetic Ni and the adjacent antiferromagnetic NiO would otherwise result in a shift of the hysteresis loop. Again, this indicates that the samples have no significant oxidization during and after the preparation.

In conclusion, a self-assembled network of pure Ni nanochains has been successfully prepared by a simple solution-phase method. Our synthetic approach has the virtues of simplicity, high yield, product stability, and generality for metallic systems. The uniform Ni nanochains are oriented and fused together like a bracelet with little lattice mis-orientation and apparent boundary. A significantly enhanced magnetic coercivity has been obtained for the nanochains compared to the bulk metal. The oriented attachment chain growth mechanism has been proposed for the formation of the unique nickel nanochain network structures prepared in solution. The excellent stability, the uniform size, the hierarchical self-assembled structure, and the peculiar magnetic properties of the bracelet-like metal nanochains lend a model system for fundamental investigations and promising applications in various fields of nanotechnology.

This project was supported by the National Natural Science Foundation of China (No. 20373004). L. Guo thanks BUAA for financial support through the Outstanding Youth Award (I). SY acknowledges support from the Research Grants Council of Hong Kong and HKUST.

Notes and references

1 (*a*) S. Link and M. A. El-Sayed, *J. Phys. Chem. B*, 1999, **103**, 8410; (*b*) J. R. Nikhi and X. G. Peng, *J. Am. Chem. Soc.*, 2003, **125**, 14280; (*c*) X. Gao, K. M. K. Yu, K. Y. Tam and S. C. Tsang, *Chem. Commun.*, 2003, **24**, 2998.
2 (*a*) J. S. Bradley, B. Tesche, W. Busser, M. Maase and M. T. Reetz, *J. Am. Chem. Soc.*, 2000, **122**, 4631; (*b*) T. O. Ely, C. Amiens and B. Chaudret, *Chem. Mater.*, 1999, **11**, 526; (*c*) J. Bao, Y. Liang, Z. Xu and L. Si, *Adv. Mater.*, 2003, **15**, 1832; (*d*) S. L. Tripp, S. V. Pusztay, A. E. Ribbe and A. Wei, *J. Am. Chem. Soc.*, 2002, **124**, 7914.
3 N. Cordente, M. Respaud, F. Senocq, M. J. Casanove, C. Amiens and B. Chaudret, *Nano Lett.*, 2001, **1**, 565.
4 Y. D. Li, L. Q. Li, H. W. Liao and H. R. Wang, *J. Mater. Chem.*, 1999, **9**, 2675.
5 A. P. Alivisatos, *Science*, 2000, **289**, 736.
6 R. L. Penn and J. F. Banfield, *Geochim. Cosmochim. Acta*, 1999, **63**, 1549.
7 R. L. Penn, G. Oskam, T. J. Strathmann, P. C. Searson, A. T. Stone and D. R. Veblen, *J. Phys. Chem. B*, 2001, **105**, 2177.
8 J. F. Banfield, S. A. Welch, H. Z. Zhang, T. T. Ebert and R. L. Penn, *Science*, 2000, **289**, 751.
9 N. Vandewalle and M. Ausloos, *Phys. Rev. E*, 1997, **55**, 94.
10 L. Jiang, C. Leu and K. Wei, *Adv. Mater.*, 2002, **14**, 421.
11 R. M. Bozorth, *Ferromagnetism*, D. Van Nostrand Company, Inc., Toronto, 1951.
12 J. Nogues and I. K. Schuller, *J. Magn. Magn. Mater.*, 1999, **192**, 203.